Journal of Physics:
Conference Series

Field-testing and serviceability assessment of a lively footbridge

To cite this article: Maria Gabriella Mulas *et al* 2024 *J. Phys.: Conf. Ser.* **2647** 122005

Field-testing and serviceability assessment of a lively footbridge

Maria Gabriella Mulas[1*], Cristina Fortis[1] and Giulia Lastrico[1]
DICA, Politecnico di Milano, Piazza Leonardo da Vinci 32, 20133 Milano, Italy

mariagabriella.mulas@polimi.it; fortiscristina@gmail.com; giulia.lastrico@gmail.com

Abstract. Following a previous work, the paper describes the serviceability assessment of a footbridge over the Lambro River near Milano (Italy), based on the comparative analysis of on-field tests and of the outcome of the Hyvoss guidelines. The 3-span footbridge, for a bicycle-pedestrian mixed use, is 107 m long, 4.4 m wide and roughly symmetric about both mid-span and the longitudinal axis. A reinforced concrete (RC) deck is supported by a steel structure: two longitudinal welded I-profiles, braced in their lower part, support the transverse beams that, in turn, support the RC deck. Ambient vibration tests identified the footbridge modal properties, detecting the fundamental bending mode, with the maximum amplitude recorded at mid-span, at 1.75 Hz, well within the critical range of excitation from walking pedestrians. Hence, a series of forced vibration tests was subsequently performed, involving single pedestrians or groups of up to 12 people. Sensors, located as in AVTs, recorded footbridge acceleration, both horizontal and vertical. In all the tests, pedestrians walked in resonance conditions with the first mode frequency along straight trajectories. To excite further the first mode, their spatial configurations were symmetric about the longitudinal axis of the bridge. Difference among tests concerns not only the number of test subjects (TSs), but also their spatial configuration and/or the TSs involved in each test. The comparison among tests sharing similar spatial configurations, with TSs either in a row or in a column, allows a serviceability assessment directly from the experimental footbridge response. The numerical analyses are based on a FE model previously developed, showing an excellent reproduction of the first bending mode, but a poor simulation of the second torsional mode. The outcome of the analyses performed according to HiVoSS guideline is in good agreement with the experimental results, in spite of the very low crowd density of the on-field tests and the unsatisfactory reproduction of the torsional mode within the FE model.

1. Introduction

In the last two decades, research studies on bridges have developed along different but interconnected lines. The availability of advanced testing procedures and sensors favored the adoption of dynamic testing of bridges for several purposes, as in the identification of dynamic properties in proof tests, validation of finite element (FE) models, and detection of excessive vibration for lively footbridges [1]-[5]. New concepts of the usage of space in cities and rural areas made for the widespread adoption of footbridges. For aesthetic reasons, their structural conception is often characterized by significant slenderness, making them prone to excessive vibration [6]. For this reason, a significant amount of research work has been devoted to the problem of their serviceability assessment [7], because slender structures are also prone to a modification of modal properties due to the increase of mass [8] and damping [9] when pedestrians are present. In addition, the problem of human-structure interaction requires to derive proper pedestrian models and analysis procedures [10], [11]. In this framework, research works encompassing all of these aspects can further current knowledge, especially when these are based on a real structure, and link together experimental and numerical data. For footbridges, the former covers field tests aiming at both the identification of modal properties and the dynamic response to human excitation. The latter encompasses validation of FE models, assessment of serviceability conditions and simulation of dynamic response under pedestrian loads.

As in other recent works [12] [13], aim of this paper is to perform the serviceability assessment of a footbridge located in Northern Italy, through both experimental and numerical studies. The research was driven by the outcome of ambient vibration tests (AVTs), performed during proof tests, that provided the footbridge modal properties. A previous work [14] showed that the first bending mode was detected at a frequency of 1.75 Hz, a critical value confirmed by a FE model, even though the frequency of the second mode, a torsional one, was not simulated successfully. The response of the footbridge to pedestrian traffic was determined through on-field tests, with 52 groups of pedestrians walking at the 1st mode frequency [14]. Based on the same experimental data, numerical studies in this work encompass the assessment of serviceability conditions in accordance with the European guidelines HiVoSS [15]. The experimental counterpart of the numerical assessment adopts the results of the forced vibration tests with walking pedestrians.

In the following, Section 2 describes the case study and the results of the structural identification. Section 3 sets out the serviceability analysis according to [15]. Section 4 describes the arrangement of field tests with walking pedestrians and the experimental assessment for vertical accelerations. A few conclusions are drawn in Section 5.

2. Footbridge description

Figure 1 shows the footbridge overpassing the Lambro River (municipality of Cerro al Lambro, Italy) and running parallel to a historical but still operating 3-arch masonry Canal Bridge dating back to 1806. The total length of 107 m is subdivided into a central span, 58 m long, and two side spans, each 24.5 m long. The constant width is equal to 4.4 m.

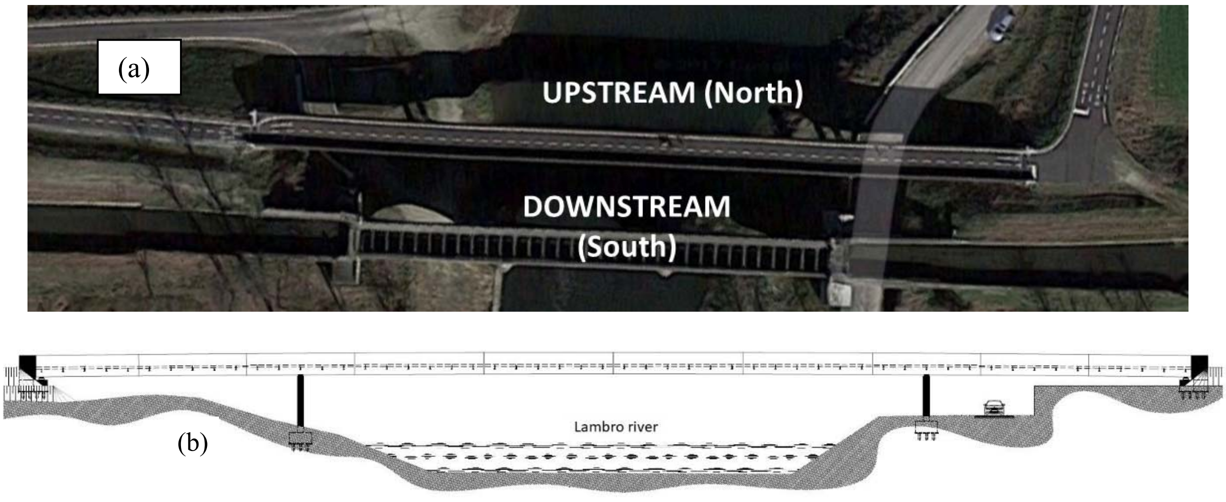

Figure 1. Lambro footbridge: (a) aerial view; (b) side view (adapted from [14]).

At the two sides of the footbridge, 2 m high welded longitudinal I-beams provide the primary structure. The two identical beams are subdivided in ten on-site welded segments, respecting symmetry about the transverse axis at mid-span. Figure 2a shows: the cross brace system, made of steel L90×8 profiles bolted, every 2 m and on a width of 4.4 m, at the bottom flange of the longitudinal beams; the transverse beams and the secondary beam, an IPE100, connecting the mid-span of transverse beams to avoid buckling phenomena. Figure 2b presents a typical cross-section. Transverse beams are spaced 2 m apart and made of IPE240 steel profile in the central span and of HEA240 on the intermediate supports and at the side spans. Transverse beams connect the longitudinal beams and support the deck where a reinforced concrete (RC) slab, with an overlying bituminous conglomerate pavement, is cast on a metal corrugated sheet. The deck has an inclination of 2% to allow rainwater to drain into a circular PVC drainage channel placed on one side only. Two pairs of circular RC columns, diameter 85 cm, provide the intermediate support (Figure 1b). The height of columns is 6.9 m on the right and 5.5 m on the left of the up-stream side, respectively. The foundation of the columns is on piles. At all supports, the bottom flange of longitudinal beams rests on elastomeric bearings SI-H 300/52 (diameter 300 mm, height 52 mm), that in turn rest on a RC 45×45 cm pier cap, 20 and 28 cm high on the upstream and downstream side, respectively.

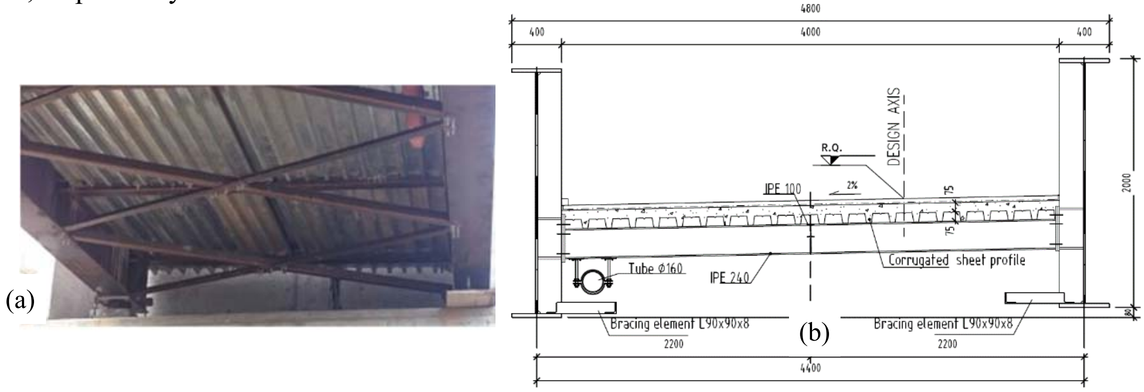

Figure 2. Lambro footbridge: (a) view from below; and (b) cross-section (adapted from [18]).

With the same A 75/P750 corrugated sheet profile, two cross-sections of the deck are realized. In the central span, the sheet thickness is 0.7 mm and the cast in situ slab is 75 mm thick, for a total deck thickness of 150 mm. At the two ends, for a length of 4.5 m from the abutments, the sheet thickness is 1.5 mm and the cast in situ slab is 305 mm thick for a total thickness of 380 mm. In these zones, the metal sheet is directly connected to the lower flanges of the I-profiles. A 10 mm thick waterproof sheath is interposed between the deck and a 30 mm thick concrete pavement. Their total weight is 1.2 kN/m^2.

All steel profiles are made of S335 steel, having ultimate strength f_u =510 MPa and yield strength f_y =335 MPa. Corrugated sheet is made of S235 steel, having f_u =360 MPa and f_y =235 MPa. Deck is made of concrete of class C30/37, with Young's modulus E_c=33.0 GPa, characteristic strength f_{ck} =30.7 MPa and design strength f_{cd} =17.4 MPa. The class of concrete for columns is C32/40, having Young's modulus E_c=33.6 GPa, characteristic strength f_{ck} =33.2 MPa and design strength f_{cd} =18.8 MPa. Further details on the footbridge geometry can be found in [16], [17].

2.1. Experimental modal properties through structural identification

Ambient vibration tests (AVTs) were performed to evaluate the footbridge dynamic properties. Figure 3 shows the accelerometer layout adopted in the experimental campaign. Only vertical sensors A1-A10 were installed on the main side beams during AVTs.

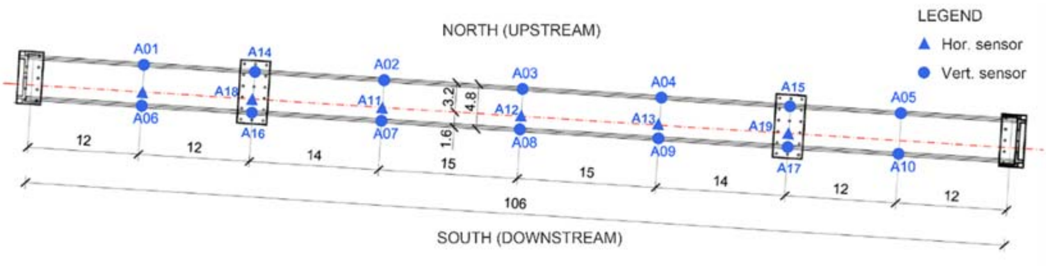

Figure 3. Accelerometers layout for the experimental campaign.

Two techniques implemented in the commercial software ARTeMIS [18], namely the Frequency Domain Decomposition (FDD) [19] and the data-driven Stochastic Subspace Identification (SSI-data) [20] provided practically coincident values of natural frequencies and modal damping ratios, listed in

Table 1. Figure 4 shows the measurement-based mode shapes for the first three modes identified using the SSI-data technique. Further details on AVTs can be found in [14].

Table 1. Summary of the identified modal parameters (B=bending; T= Torsion)

Mode Id.	1 (B)	2 (T)	3 (B)	4 (B)	5 (T)	6 (B)	7 (T)	8 (B)	9 (T)
f_{FDD} (Hz)	1.748	2.910	4.668	6.660	6.797	7.441	9.954	10.190	10.030
f_{SSI} (Hz)	1.749	2.912	4.675	6.676	6.862	7.443	9.956	10.190	11.060
ζ_{SSI} (%)	0.135	0.758	0.249	1.001	3.084	1.389	1.373	1.774	1.172

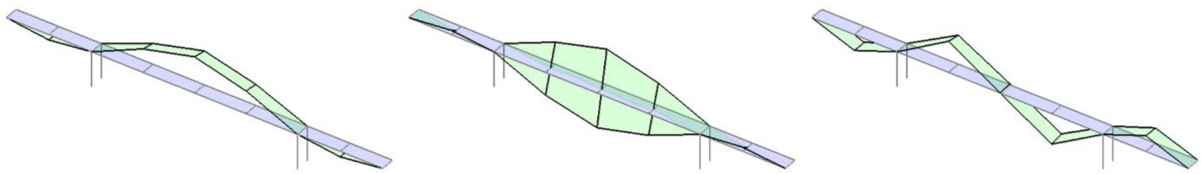

Figure 4. Vibration modes 1 to 3 identified from AVTs (SSI-data) (from [14]).

3. Serviceability analysis (Hivoss)

The numerical assessment of the serviceability conditions follows the HiVoSS Guideline [15], developed within the SYNPEX European research project [21]. The procedure, in the framework of the *performance-based design*, aims at providing a selected class of comfort for the relevant traffic class. As well documented in the literature, the ground reaction force, i.e. the load transferred by each pedestrian in a step, can be simulated as the sum of Fourier harmonic components [22]. Hence, the assessment of comfort conditions is based on a harmonic analysis at resonance conditions, under a conventional load pattern depending on both the mode shape and the traffic class, for the modes whose frequency falls in a critical range. This range is 1.25 Hz $\leq f_i \leq$ 2.30 Hz for vertical and longitudinal vibration, with the upper limit set to 4.6 Hz, when the 2nd harmonic of the pedestrian load is relevant for the bridge response. The range for lateral vibration is 0.5 Hz $\leq f_i \leq$ 1.2 Hz.

The control parameter is the peak value of either the vertical a_v or the lateral a_l acceleration, to be compared with the limit values of comfort classes. HiVoSS lists four classes: maximum comfort CL1 (a_v < 0.5 m/s^2), medium comfort CL2 (0.5< a_v <1 m/s^2), minimum comfort CL3 (1< a_v <2.5 m/s^2) up to unacceptable discomfort of CL4 (a_v >2.5 m/s^2). Five classes of traffic range from very weak traffic (TC1) to a very dense one (TC5) corresponding to persistent, transient and accidental or exceptional design situations, as the one for the bridge inauguration. Since the bridge connects two cycle routes in a rural area, only TC1 (very weak traffic) and TC2 (weak traffic) classes are considered. Defining P as the force component of a single pedestrian, given the deck length L and width B, the former corresponds to a group of 15 pedestrians, with a pedestrian density $d = 15P/BL \simeq 0.035$ P/m^2, the latter to d equal to 0.2P/m^2. In both situations, pedestrians can move freely on the bridge. Vibration serviceability criteria are satisfied if the computed acceleration values do not exceed the limits of the selected comfort classes.

The pedestrian load, mainly of random nature and affected by both inter- and intra-subject variability, is defined by a deterministic, uniformly distributed, harmonic load $p(t)$ representing an equivalent pedestrian stream:

$$p(t) = P \cdot cos\,(2\pi f_s t) \cdot n' \cdot \psi \qquad [N/m^2] \tag{1}$$

In (1), $Pcos\ (2\pi f_s t)$ is the harmonic load from a single pedestrian. The P value takes into account the dynamic load factor, i.e. the coefficient of the Fourier series (P = 280 N for vertical load). The direction of the harmonic load is the same as of the half-waves characterizing the mode shapes associated to the natural frequency considered in the dynamic analysis. The step frequency f_s is assumed equal to any of the footbridge natural frequencies under consideration. The reduction coefficient ψ (values in [15]) takes into account the probability that the footfall frequency approaches the critical range of natural frequencies under consideration. The parameter n' is the equivalent number of perfectly synchronised pedestrians on the loaded surface S. The definition of n' for the case of sparse crowd, with pedestrians moving freely on the footbridge, is a function of the structural damping ratio ξ (here equal to 0.4%, as suggested by HiVoSS for steel bridges), the loaded surface S and the number of pedestrians n on the surface ($n = S{\cdot}d$):

$$n' = \frac{10.8\sqrt{\xi \cdot n}}{S} \qquad \left[\frac{1}{m^2}\right] \tag{2}$$

The assessment of the serviceability conditions was performed in the extended critical range in [16], on the optimized FE model in [14]. Four modes belong to the critical interval: the counterpart of the first two experimental modes (4th and 6th), and two purely numerical modes containing a vertical component, 5th (lateral/torsional, f_5 = 1.90 Hz) and 7th (lateral/flexural, f_7 = 3.68 Hz). Maximum values, tracked at the position of accelerometers (Figure 5), are shown in Figure 6 for the two classes of traffic.

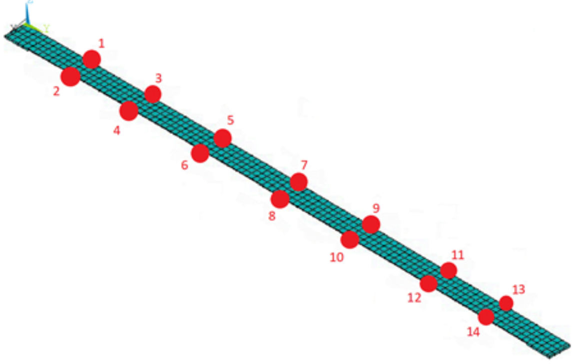

Figure 5. Position and numbering of nodes where extreme values of acceleration are tracked.

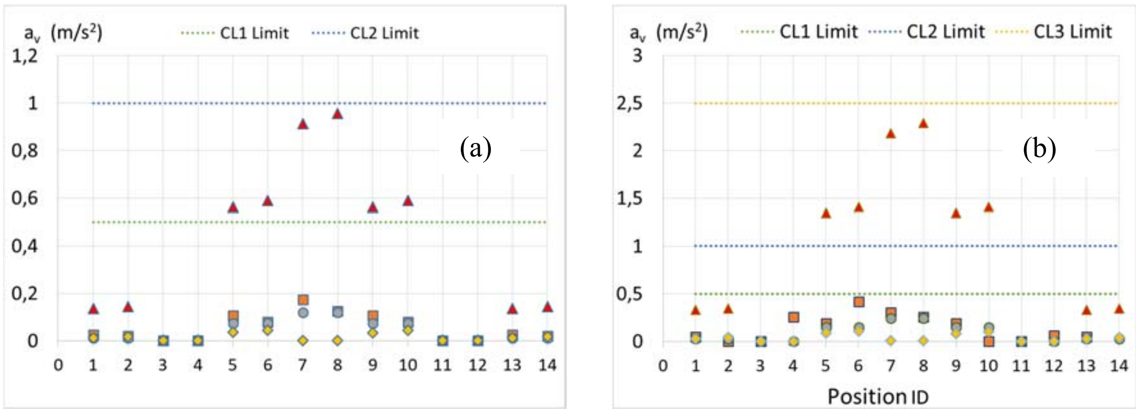

Figure 6. Results of harmonic analysis for the selected traffic classes: (a) TC1; (b) TC2. Legenda: red triangle, orange square, grey circle and yellow romboids correspond to numerical modes 4, 5, 6 and 7, respectively [16].

Extreme values are due to the first bending mode and are distributed according to its mode shape, with a maximum at mid-span. In each cross-section of the central span, downstream values exceed upstream ones. For the first mode, nodes in central spans are outside CL1 but within CL2 for traffic class TC1, while the limit of class CL3 is almost reached for TC2. The result is acceptable, due to the low probability of the occurrence of TC2 for the bridge. The response to the first torsional mode is within the limit of CL1 and that to purely numerical modes is negligible. Results for lateral acceleration, not reported here for the sake of compactness, are within CL1 for TC1 and within CL2 for TC2.

4. Forced vibration tests

Forced vibration tests with walking pedestrians ([14], [16]) were performed after the proof tests, to assess the serviceability conditions of the bridge crossed by groups of different numbers and configuration of pedestrians. Table 2 presents the ID, sex, mass *M* and height *H* of the twelve volunteers involved in the tests. The age of TS5 and TS8 is in the range 50-60. The remaining TSs have an age between 22 and 30.

Table 2 – General data of test subjects (TS) involved in the walking tests.

ID	TS1	TS2	TS3	TS4	TS5	TS6	TS7	TS8	TS9	TS10	TS11	TS12
Sex	M	M	F	F	M	F	F	M	M	M	M	M
M [kg]	65	86	59	53	70	65	62	84	76	72	73	70
H [cm]	172	182	164	158	181	173	170	177	185	183	175	175

Fifty-two tests were performed, adopting 17 different space configurations shown in Figure 7. Each TS walked alone. Groups of 2, 3 and 4 pedestrians were either in a longitudinal row or in a transverse row. For the last case, a configuration in two rows was added. Groups of 6 and 8 pedestrians were either in a longitudinal row or in two transverse rows. Groups of 12 pedestrians adopted five spatial configurations, one with a longitudinal row and four with a varying number (2, 3, 4 and 6) of transverse rows. All the configurations respect symmetry about, or are aligned on, the longitudinal axis.

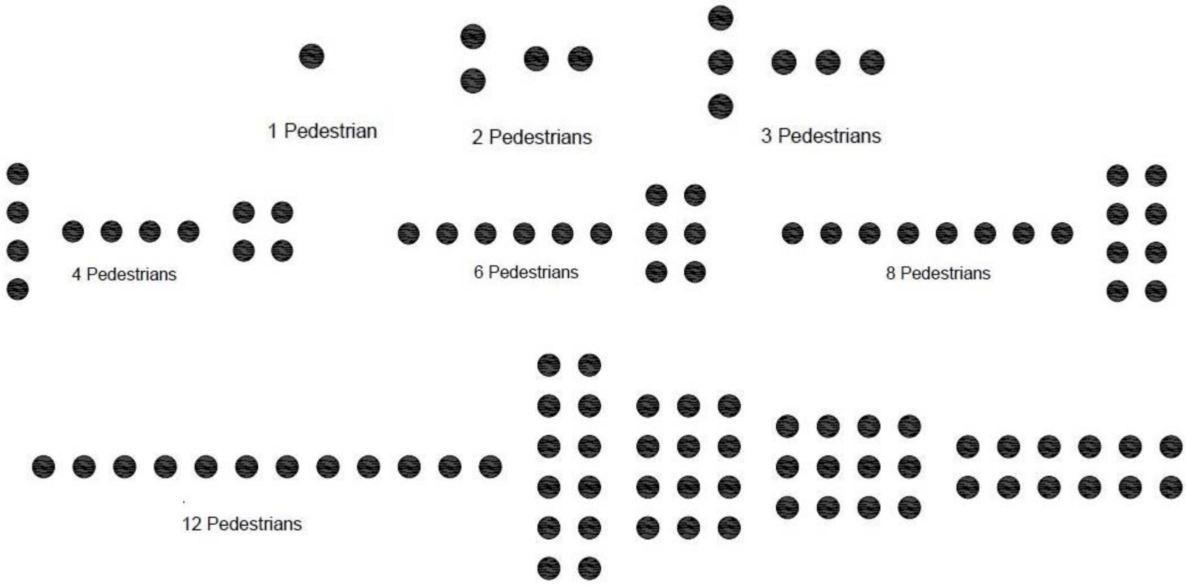

Figure 7. Spatial configurations of pedestrians. From top to bottom and from left to right, configurations with 1, 2, 3, 4, 6, 8 and 12 pedestrians.

Table 3 shows the total number of tests for each number of pedestrians, differing in space and in the TSs involved. Forty tests concerned groups of two or more pedestrians. In longitudinal direction, pedestrians were spaced apart at a target distance of 60 cm. In transverse direction, inter-distance was not constant, depending on the number of pedestrians involved. For each space configuration of a given group of pedestrians, at least two tests were performed varying the TSs involved.

Table 3. Number of configurations adopted for each number of pedestrians crossing the bridge.

Pedestrians #	1	2	3	4	6	8	12
Configurations	12	6	6	9	4	4	11

To assess the extreme values of the bridge response, the tests layout was conceived to excite mainly the first bending mode. The target walking frequency was set to 1.75 Hz and only symmetric spatial configurations were assumed, to minimize the contribution of torsional modes. A preliminary session defined the best way to impose a footstep rhythm between a metronome and a song with main beat at 1.75 Hz (*Stayin' Alive* by *Bee Gees*). The song showed to be more effective to maintain a natural but synchronized gait and was used in all the subsequent tests.

The bridge vibrations were recorded by 17 accelerometers (layout in Figure 3), located on the top flange of longitudinal beams. The measurement set-up adopted the high sensitivity accelerometers and the data acquisition system of the AVTs. Vertical sensors from A1 to A10 are in the same positions as for operational modal analysis. Three horizontal sensors (A11/12/13) were added in the central span. Four vertical (A14/15/16/17) and two horizontal (A18 and A19) sensors are located at the intermediate supports, providing information on the time of passage of pedestrians on these cross-sections.

A single record with multiple channels corresponds to each of the 52 tests. Pedestrians crossed the whole bridge, entering from the left side in Figure 1a. Signal recording lasted from a few instants before the entrance of pedestrians on the bridge up to a significant decay of free vibrations following the transit. Each TS gave a heel strike while entering the bridge, to mark the time instant of initiating crossing. As a general trend, the recorded response reflects the quasi-symmetry of the bridge. Downstream records are similar but slightly larger than upstream ones, consistently with the result of the numerical assessment. Similarly, records on the first and second half of the bridge almost overlap, but larger accelerations are found on the second half, indicating a resonance phenomenon increasing with the elapsed time from the entrance. For the sake of brevity, only vertical accelerations are analyzed in the following.

4.1. Peak values as a function of the number of crossing pedestrians

First, extreme values of vertical acceleration are evaluated as a function of the number of TSs involved in the tests, regardless to the space configuration. Results of the twelve single pedestrian tests in terms of extreme values recorded by downstream sensors, not shown here for the sake of brevity, indicate that peak values in A6 and A10 are similar but not equal. With some exception, values in A10, at the end of the bridge crossing, exceed those in A6, at the bridge entrance, coherently with a resonance phenomenon building up during the crossing. Sensor A8 at mid-span (the antinode of the first bending mode) detects the overall extreme value for this group of tests, equal to 0.30 m/s^2. The value is within the comfort range according to HiVoSS Guideline [15], but reached with a single pedestrian. The minimum peak value in A8, around 0.06 m/s^2, indicates a large variability in extreme values produced by different TSs, also apparent in the dispersion about the average of peak values.

For the same downstream sensors, Figure 8 presents peak values in tests with multiple pedestrians, as a function of the number of crossing pedestrians. Dotted lines represent the average of peak values. Figure 8a depicts results for group of two, three and four TSs. The overall extreme value for this group of tests is about 0.9 m/s^2, close to the limit of comfort class CL2, but obtained with just three pedestrians. The average values for groups of three and four are very close, but are larger for the group of three, due to a test with very large accelerations. Figure 8b shows the results for the larger groups of six, eight and twelve people. Average of peak values of vertical acceleration increase with the number of pedestrians. The overall extreme value in A8 slightly exceeds 2 m/s^2 in a test with a compact configuration of 12 TSs in three transverse rows of four pedestrians. This value, similar to that predicted by [15] for TC2, is outside CL2 comfort class, but cannot be considered as representative of the serviceability conditions of the footbridge, given the quite severe configuration that produced it.

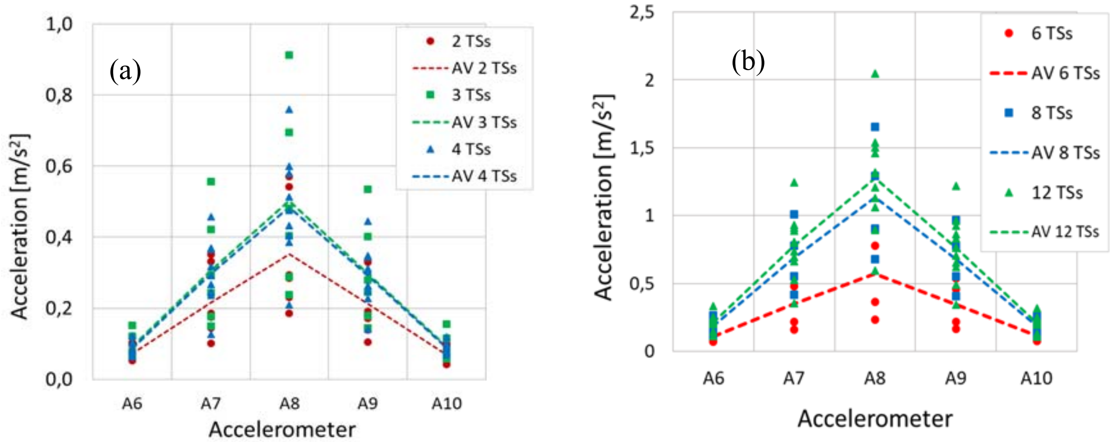

Figure 8. Peak and average (dotted lines) of peak values of acceleration for different configurations: (a) groups of 2, 3 and 4 TSs; (b) groups of 6, 8 and 12 TSs.

4.2. Peak values as a function of pedestrians' configuration

The bridge performance under ordinary conditions is assessed through tests with the simplest configuration of pedestrians aligned along a single row, in terms of the acceleration peak value at A8. The configuration with one longitudinal row is adopted for all the groups, with a number of TSs ranging from one to 12 (Figure 7). Only groups up to 4 TSs are present in configurations in a single transverse row, where TSs excite the bridge through the same modal shape coordinate. Since for each configuration more than one test was performed, with different TSs, both peak and average values are depicted in Figure 9a, b for pedestrians in a longitudinal and transverse row, respectively. In the first case, the peak value reaches a maximum around 0.9 m/s^2 with six pedestrians and then slightly decreases as the number of TSs increases. Average values show a similar but more regular variation, with a maximum for 8 TSs and a close but lower value for 12 TSs. The second case shows a similar trend, with the maximum due to 3 TSs. The curve of average values in this case indicates a lower level of peak acceleration, but it is noteworthy that the peak acceleration reaches 0.9 m/s^2, as for the case of the longitudinal row.

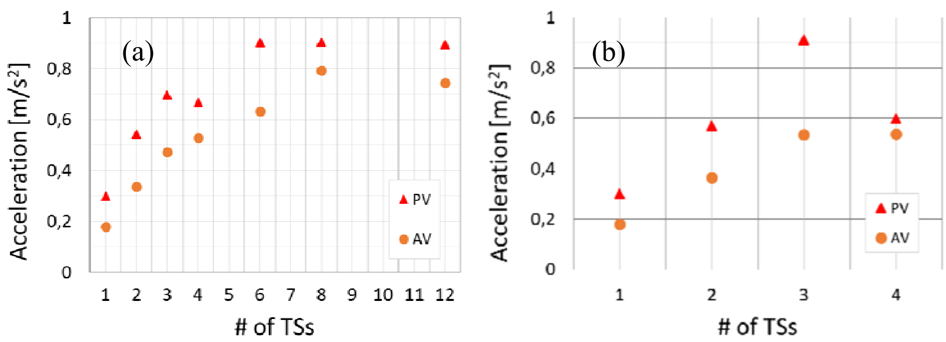

Figure 9 – Sensor A8, peak (PV) and average (AV) values of vertical acceleration for pedestrians in in a single: (a) longitudinal row; (b) transverse row.

Figure 10a,b shows the results for configurations with TSs aligned in multiple transverse and longitudinal rows. For the first case (Figure 10a), transverse rows of two (with 1, 2 or 6 rows), three (with 1, 2 or 4 rows) and four (with 1, 2 or 3 rows) TSs are considered. The second case (Figure 10b) encompasses longitudinal rows of two (with 1, 2, 3, 4 and 6 rows), three (with 1 or 4 rows), four (with 1 or 3 rows) and six (with 1 or 2 rows) TSs. For each configuration, the average of peak values in tests sharing the same configuration is plotted vs the number of TSs in the test. The peak values, for both types of configuration, increase as the number of TSs in the test, falling well outside the comfort zone (up to 1.8 *m/s*^{2}) for the most compact configuration, where 12 TSs occupy a limited surface on the bridge.

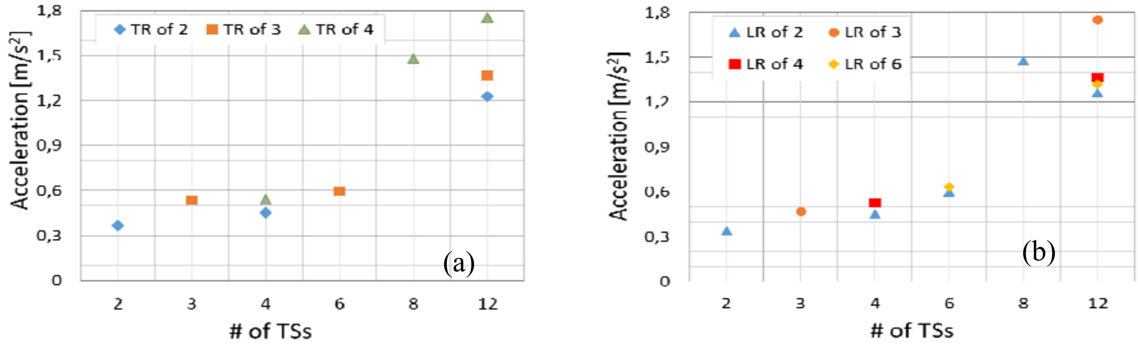

Figure 10. Average of peak values of acceleration for tests sharing the same configurations of TSs: (a) in transverse rows; (b) in longitudinal rows.

To further investigate this aspect, Figure 11a,b,c shows the time history at downstream sensors A6 to A10, for three tests with 12 TSs in one, two and three longitudinal rows, respectively. As the number of TSs in each longitudinal row decreases, the peak acceleration increases.

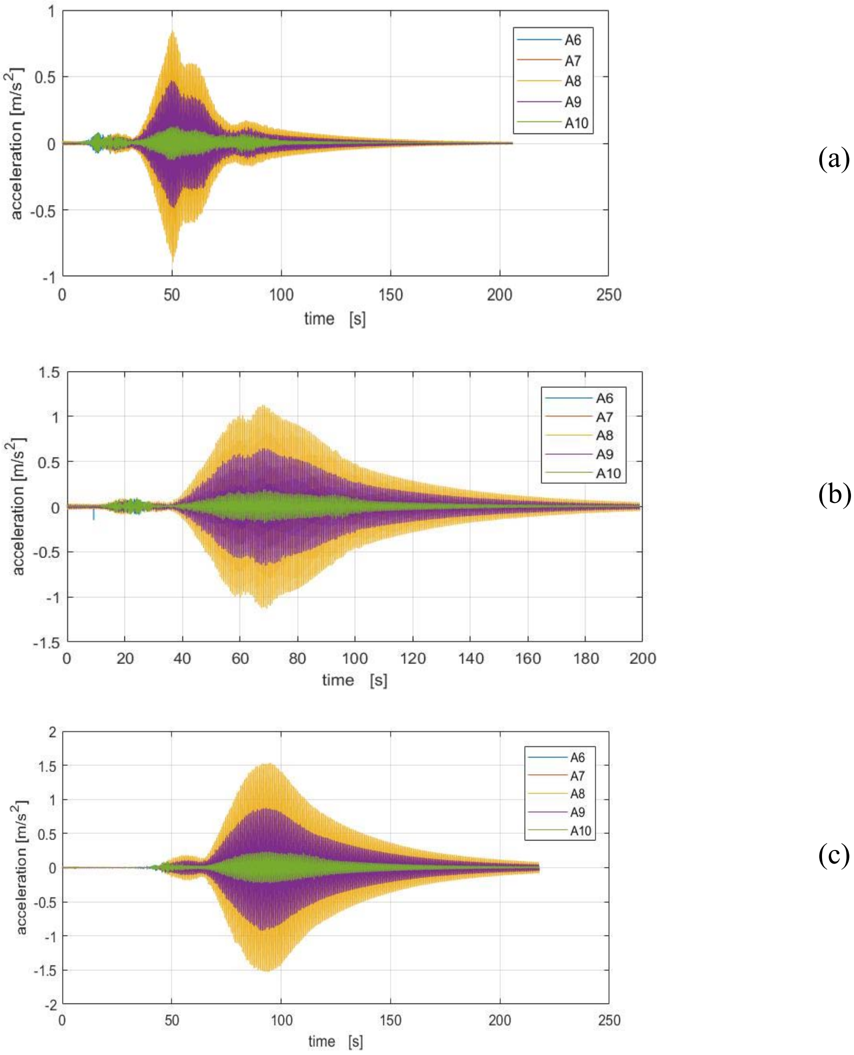

Figure 11. Time history for three tests with 12 TSs in different configurations: (a) Test 55, TSs in a longitudinal row; (b) Test 61, TSs in two longitudinal rows; (c) Test 64, TSs in three longitudinal rows.

The effect of higher modes, well visible in Figure 11a (peak value around 0.9 m/s^2), is still present in Figure 11b, with peak acceleration around 1.1 m/s and almost vanishes in Figure 11c, when peak value is around 1.5 m/s^2. With 12 walking TSs, the level of their synchronization will depend on the length of row, being larger in compact configurations, when synchronization among TSs is easier. Peak values increase as the role of the first bending mode dominates the bridge response.

Figure 12 shows the response spectra for the test in Figure 11b, for two time intervals, namely 0-20 s, corresponding to the initial part of the test (Figure 12a), and 50-70 s, covering the time interval in which TSs cross the mid-span (Figure 12b). In each part of the figure, plots refer to sensors A6, A7 and A8 in the first line, and to A9 and A10 in the second line. The ten plots adopt the same scale in abscissa, and different scales for the ordinates, adjusted on the maximum spectrum value. Hence, the end value of the vertical axis provides a direct indication of the vibration level at the sensor. In each time interval, this increases, moving in the direction of crossing, i.e. from A6 to A8. Spectra of the couples of sensors A6, A10 and A7, A9, symmetrically placed with respect to mid-span, are quite similar in both intervals.

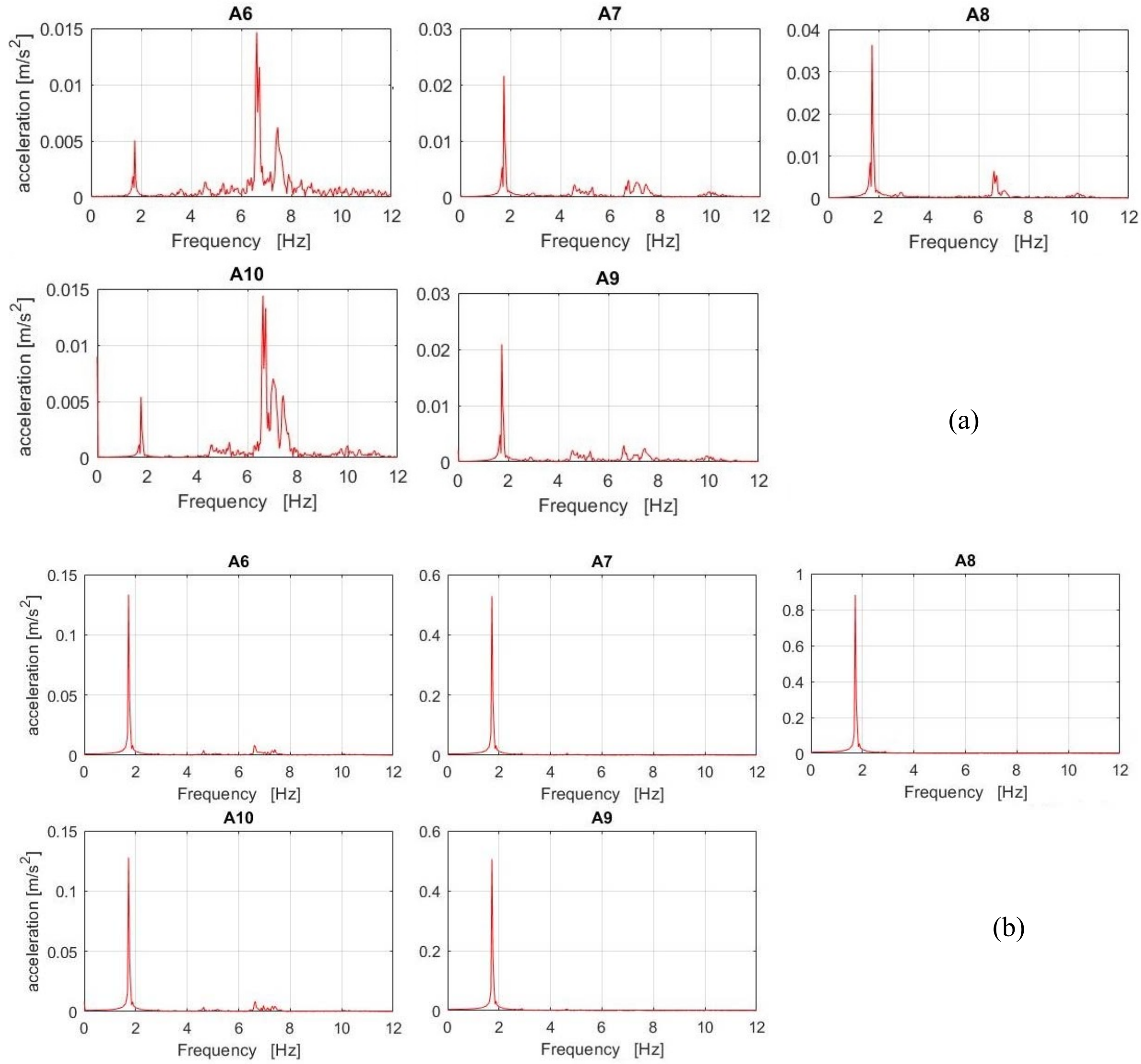

Figure 12 – Response spectra for TEST 61, 6 transversal rows of 2 TSs, at downstream sensors A6-A10: (a) time interval 0 – 20 s; (b) time interval 50 - 70 s.

Largest values are consistently detected at mid-span (A8) where the higher modes effect is not large enough to be detected at the scale of the plot. Comparison of spectra in the same sensor for the two time intervals points out the increasing effect of the first mode as the resonance phenomenon builds up. The broader range of A6 spectrum in Figure 12a could originate from the initial heel strike of TSs.

5. Conclusions

This paper presents an experimental and numerical research work performed on a footbridge located in Northern Italy. The work stemmed from the AVT's carried out as a part of proof tests. The identification of the fundamental mode at the critical frequency of 1.75 Hz was the origin of a second experimental campaign, performed one year later within a sponsored research program, in which the bridge vibration due to groups of pedestrians walking at the first mode frequency was recorded.

The numerical assessment of serviceability conditions carried out for very weak and weak traffic classes, resulted in peak values of vertical acceleration at mid-span around 0.9 m/s^2 and 2.3 m/s^2, within the class of medium and minimum comfort, respectively [15]. The result is acceptable seeing the bridge usage. The experimental assessment was performed extracting selected results from the second experimental campaign, with groups from 1 to 12 pedestrians. Since pedestrians walk at the same frequency of the first mode, forced vibration tests are directly comparable to numerical results, obtained from harmonic analyses in resonance with the first mode. In both cases, peak values of vertical acceleration, found at mid-span, increase as the number of pedestrians increases; downstream values are slightly larger than upstream ones.

A wide scatter affects experimental results when the same configuration is adopted for different TSs. Peak values due to a 12-TS configuration are close to those for the weak traffic class, in which a much larger number of pedestrians is spread uniformly over the bridge surface instead of being concentrated on a limited area. The results for the very weak traffic class are well approximated by those due to pedestrians in a single row, either longitudinal or transverse, testifying that both the numerical analysis and properly designed and analyzed experimental tests produce a reliable serviceability assessment. Finally, a selected group of signals due to 12 pedestrians configurations in both time and frequency domain is analyzed. The size of longitudinal rows governs the response, with an increasing level of vibration as the rows size decreases, favoring the pedestrians' synchronization and increasing the load on the zones with the largest values of modal shape deformation. Response spectra highlight the building of the resonance phenomenon with the elapsed time, and the overwhelming effect of the first bending mode in the central part of the footbridge at the time pedestrians are around mid-span. Results fully justify the "fall out" command usually given, also in the distant past, to soldiers crossing a bridge.

From the experimental point of view, further studies will address the bridge response in non-resonance conditions. A process of model updating is still necessary to correctly simulate also the frequency of the second torsional mode. The availability of both a validated FE model, providing a reliable numerical model of a real structure in the coupled problem of human-structure interaction, and of the experimental tests, lay the basis to develop and validate modelling strategies for pedestrians as mechanical systems, moving with a given gait.

Acknowledgements

This work is based on the MS theses in Civil Engineering, Politecnico di Milano, of C. Fortis and G. Lastrico, under the guidance of the first Author. The contribution of A. Cigada in the forced vibration tests is gratefully acknowledged. The first Author acknowledges the financial contribution of Italian MIUR under grant PRIN 2015-2018, Project 2015TTJN95, "Identification and monitoring of complex structural systems".

References

[1] Caetano E, Cunha Á, Magalhães F and Moutinho C 2010 Studies for controlling human-induced vibration of the Pedro e Inês footbridge, Portugal. Part 1: Assessment of dynamic behaviour, *Engng Struct*, (32), 1069-1081.

[2] Benedettini F and Gentile C 2011 Operational modal testing and FE model tuning of a cable-stayed bridge, *Engng Struct*, (33), 2063-2073.

[3] Gheitasi A, Ozbulut OE, Usmani S, Alipour M and Harris DK. 2016 Experimental and analytical

vibration serviceability assessment of an in-service footbridge, *Case Studies in Nondestructive Testing and Evaluation*, (6), 79-88.

[4] Lai E, Gentile C and Mulas MG 2017 Experimental and numerical serviceability assessment of a steel suspension footbridge, *J. of Constructional Steel Research*, (132), 16-28.

[5] Ribeiro de Silva IA, and Santos de Silva G 2018 Experimental and numerical dynamic structural analysis of footbridges when subjected to pedestrians walking loads, *J. of Civil Struct Health Monitoring*, 8: 585-595, 2018.

[6] Dallard P, Fitzpatrick A, Flint A, Bourva S, Low A, Ridsdill R and Willford M 2001 The London Millenium footbridge, *The Structural Engineer*, 79(22), 17-33.

[7] Van Nimmen K, Lombaert G, De Roeck G and Van den Broeck P 2014 Vibration serviceability of footbridges: evaluation of current codes of practice, *Engng Struct*, (59), 448-461.

[8] Busca G, Cappellini A, Manzoni S, Tarabini M and Vanali M .2014 Quantification of changes in modal parameters due to the presence of passive people on a slender structure, *J. of Sound and Vibration*, (333), 5641-5652.

[9] Georgakis CT and Jørgensen NG 2013 Change in Mass and Damping on Vertically Vibrating Footbridges Due to Pedestrians. In: *Cunha A. (eds) Topics in Dynamics of Bridges, Vol. 3. Proc. Society for Exper Mech Series*. Springer. https://doi.org/10.1007/978-1-4614-6519-5_4.

[10] Caprani CC and Ahmadi E 2016 Formulation of human-structure interaction system models for vertical vibration, *J. of Sound and Vibration*, (377), 346-367.

[11] Mulas MG, Lai E and Lastrico G 2018 Coupled Analysis of Footbridge-Pedestrian Dynamic Interaction, *Engng Struct*, 176C, 127-142.

[12] Rodríguez-Suesca AE, Gutiérrez-Junco OJ and Hernàndez-Montes E 2022 Vibration performance assessment of deteriorating footbridges: A study of Tunja’s public footbridges. *Engng Struct* 256, 113997.

[13] Hawryszków P and Biliszczuk J 2022 Vibration Serviceability of Footbridges Made of the Sustainable and Eco Structural Material: Glued-Laminated Wood. *Materials* 15 https://doi.org/10.3390/ma15041529..

[14] Cigada A, Gentile C, Lastrico G and Mulas MG 2020 Measuring the dynamic response of a lively footbridge to ambient and walking excitation. *Proceedings of XI EURODYN*.

[15] Research Fund for Coal and Steel 2008 HiVoSS: Design of footbridges, *Guideline EN03*.

[16] Lastrico G 2017 Studio numerico e sperimentale della risposta dinamica di una passerella pedonale, *MS Thesis in Civil Engng*, Politecnico di Milano, 2017 (in Italian).

[17] Fortis C 2021 Studio numerico e valutazione sperimentale delle proprietà dinamiche di una passerella pedonale. *MS Thesis in Civil Engng*, Politecnico di Milano (in Italian).

[18] SVS, ARTeMIS Extractor 2011. http://www.svibs.com/, 2012.

[19] Brincker R, Zhang LM and Andersen P 2000 Modal identification from ambient responses using Frequency Domain Decomposition, *Proc of the 18th IMAC*.

[20] Peeters B and De Roeck G 1999 Reference-based stochastic subspace identification for output-only modal analysis, *Mechanical Systems and Signal Processing* 13(6), 855-878.

[21] European Commission, Research Fund for Coal and Steel 2008 SYNPEX: advanced load models for synchronous pedestrian excitation and optimised design guidelines for steel footbridges, Final Report.

[22] Živanović S, Pavic A, Reynolds P 2005 Vibration serviceability of footbridges under human-induced excitation: a literature review, *J. Sound Vib*. 279 (1-2) 1-74.